



Low-cost Engineering of Laser Rods and Slabs with Liquid Phase Epitaxy

by Jeffrey O. White and Carl E. Mungan

ARL-TR-5741

September 2011

NOTICES

Disclaimers

The findings in this report are not to be construed as an official Department of the Army position unless so designated by other authorized documents.

Citation of manufacturer's or trade names does not constitute an official endorsement or approval of the use thereof.

Destroy this report when it is no longer needed. Do not return it to the originator.

Army Research Laboratory

Adelphi, MD 20783-1197

ARL-TR-5741

September 2011

Low-cost Engineering of Laser Rods and Slabs with Liquid Phase Epitaxy

Jeffrey O. White

Sensors and Electron Devices Directorate, ARL

Carl E. Mungan

Physics Department, U.S. Naval Academy

REPORT DOCUMENTATION PAGE				Form Approved OMB No. 0704-0188	
<p>Public reporting burden for this collection of information is estimated to average 1 hour per response, including the time for reviewing instructions, searching existing data sources, gathering and maintaining the data needed, and completing and reviewing the collection information. Send comments regarding this burden estimate or any other aspect of this collection of information, including suggestions for reducing the burden, to Department of Defense, Washington Headquarters Services, Directorate for Information Operations and Reports (0704-0188), 1215 Jefferson Davis Highway, Suite 1204, Arlington, VA 22202-4302. Respondents should be aware that notwithstanding any other provision of law, no person shall be subject to any penalty for failing to comply with a collection of information if it does not display a currently valid OMB control number.</p> <p>PLEASE DO NOT RETURN YOUR FORM TO THE ABOVE ADDRESS.</p>					
1. REPORT DATE (DD-MM-YYYY) September 2011		2. REPORT TYPE		3. DATES COVERED (From - To) March 2009 to March 2011	
4. TITLE AND SUBTITLE Low-cost Engineering of Laser Rods and Slabs with Liquid Phase Epitaxy				5a. CONTRACT NUMBER	
				5b. GRANT NUMBER	
				5c. PROGRAM ELEMENT NUMBER	
6. AUTHOR(S) Jeffrey O. White and Carl E. Mungan				5d. PROJECT NUMBER	
				5e. TASK NUMBER	
				5f. WORK UNIT NUMBER	
7. PERFORMING ORGANIZATION NAME(S) AND ADDRESS(ES) U.S. Army Research Laboratory ATTN: RDRL-SEE-O 2800 Powder Mill Road Adelphi, MD 20783-1197				8. PERFORMING ORGANIZATION REPORT NUMBER ARL-TR-5741	
9. SPONSORING/MONITORING AGENCY NAME(S) AND ADDRESS(ES) HEL-JTO 801 University Bldg. SE, Suite 209 Albuquerque, NM 87106				10. SPONSOR/MONITOR'S ACRONYM(S)	
				11. SPONSOR/MONITOR'S REPORT NUMBER(S)	
12. DISTRIBUTION/AVAILABILITY STATEMENT Approved for public release; distribution unlimited.					
13. SUPPLEMENTARY NOTES					
14. ABSTRACT We investigated the use of a liquid phase epitaxial (LPE) coating to improve the performance of a rod or slab laser. A single crystal erbium-doped yttrium aluminum garnet (Er:YAG) rod coated with undoped YAG, and an uncoated sample were procured, then compared on the basis of threshold and slope efficiency measurements. The goal of the testing was to determine the minimum epitaxial thickness necessary to suppress the whispering gallery modes, which otherwise would deplete the gain in ~50% of the rod volume. We also investigated LPE growth on a ceramic sample, because state-of-the-art high power slab lasers are now ceramic. As expected, the sample turned out to be of poor optical quality; no lasing or even transmission measurements could be made.					
15. SUBJECT TERMS Rod laser, parasitic, liquid phase epitaxy, whispering gallery modes					
16. SECURITY CLASSIFICATION OF:			17. LIMITATION OF ABSTRACT UU	18. NUMBER OF PAGES 24	19a. NAME OF RESPONSIBLE PERSON Jeffrey O. White
a. REPORT Unclassified	b. ABSTRACT Unclassified	c. THIS PAGE Unclassified			19b. TELEPHONE NUMBER (Include area code) (301) 394-0069

Contents

List of Figures	iv
1. Introduction	1
2. Description	2
3. Task 1–LPE on Single Crystal Er:YAG	3
4. Task 2–Simulation	8
5. Task 3–LPE on Ceramic	13
6. Conclusion	14
7. References	15
Distribution List	16

List of Figures

Figure 1. (a) An end-pumped clad rod in a laser cavity. The laser oscillation is a mode of the cavity, the pump beam is wave guided by TIR at the outer surfaces of the rod. (b) Rod cross section showing the whispering gallery modes that occupy ~50% of the volume for the case of an unclad YAG rod immersed in water. (c) In a rod clad with undoped material, the WGM will be suppressed because the gain is zero.	2
Figure 2. Er:YAG rod, 3 mm diameter, clad with ~2 mm of undoped YAG. (left) as-grown. (right) cut and polished.	3
Figure 3. Drawing of laser head designed to accommodate rods of diameter 3–6 mm.	4
Figure 4. Laser cavity formed by high reflector, laser head, and output coupler.	4
Figure 5. Side view of rod with WGM, upconversion disk, imaging optics, and digital camera.	5
Figure 6. Images of the LPE rod face. (a) Fluorescence emitted from the rod when it is pumped at 1532 nm. The emission is transmitted through a long-wave pass filter. (b) Image taken with room light, showing the core (central darker region), cladding (with small chips), and laser head.	5
Figure 7. Geometry for measuring transmitted pump power during lasing.	6
Figure 8. Laser output power vs absorbed pump power at $R=0.98$, for clad and unclad rods.	6
Figure 9. Threshold absorbed pump power vs. output coupler reflectivity for clad and unclad rods. Data recorded on 8 Feb.	7
Figure 10. Same as figure 8, except experiment repeated on 10 Feb.	7
Figure 11. Images of the rod taken with a digital camera and electronic flash.	8
Figure 12. Projection image of the LPE rod taken with collimated 1532 nm light passing through the rod and then incident on the camera, with no focusing lens. The central hot spot is an interference effect.	8
Figure 13. Graph showing which EH_{lm} modes are supported by an 0.2 mm YAG rod in H_2O ($V = 471$).	9
Figure 14. Fields E_r , E_ϕ , H_r , H_ϕ , and S_z associated with the $HE_{1,1}$ (fundamental) mode of a 200 μ diameter YAG rod in water. The 2D integral of the Poynting vector is shown in the lower right hand graph. The diagram shows the cladding thickness required to reduce the gain by half.	10
Figure 15. Fields associated with the $EH_{1,1}$ mode of the same rod, the 2D integral of the Poynting vector, and the cladding thickness required to reduce the gain by half.	10
Figure 16. Fields associated with the $HE_{1,15}$ mode, the 2D integral of the Poynting vector, and the cladding thickness required to reduce the gain by half.	11
Figure 17. Fields associated with the $EH_{10,1}$ mode, the 2D integral of the Poynting vector, and the cladding thickness required to reduce the gain by half.	11

Figure 18. Fields associated with the $HE_{20,1}$ mode, the 2D integral of the Poynting vector, and the cladding thickness required to reduce the gain by half.	12
Figure 19. Fields associated with the $HE_{30,1}$ mode, the 2D integral of the Poynting vector, and the cladding thickness required to reduce the gain by half.	12
Figure 20. Photo of a ceramic rod from Konoshima after an attempt at liquid phase epitaxy. ...	14

INTENTIONALLY LEFT BLANK.

1. Introduction

Ruby rods were originally polished on the barrel surface in order to more efficiently transmit the light from the flash lamp. Parasitic whispering gallery modes (WGM) at the laser wavelength arose due to total internal reflection (1). For the last 40 years, WGM in rod and slab lasers have been suppressed by grinding the barrel surface (2).

With the advent of diode laser pumping, end-pumped rods and multi-kilowatt slabs were again polished on the lateral surface to waveguide the pump (3, 4). This inevitably leads to WGM, for any dopant and host, unless the coolant happens to absorb the evanescent part of the WGM, which is the case for Tm at 2 μm (5).

For yttrium aluminum garnet (YAG) immersed in cooling water, the index difference is so high that the WGM occupy 50% of the rod volume, severely depleting the gain. Coating the rod with a layer of undoped host material would presumably remove the gain for the WGM, thereby potentially doubling the output power. Early attempts to use index matching liquid failed because of degradation, and attempts to use solder glass cladding failed because of thermo-mechanical mismatch (6).

In the current generation of slabs for the joint high-power solid-state laser program (JHPSSL3), optical path distortion due to temperature non-uniformities lowers the extractable volume by $\sim 10\%$ (7). We proposed that an epitaxial layer of undoped YAG could alleviate the problem, potentially raising the slope efficiency by 10%. Adhesive-free bonding, or diffusion bonding, is not practical in this situation. In larger slabs, the gain for parasitic modes may become so high that grinding the surfaces will not be sufficient (8). An epitaxial layer may be useful for parasitic suppression in this case, as shown in previous work with slabs and disks (10). A core-doped hexagonal rod has also been fabricated by bonding (9) undoped layers to each lateral surface, and has shown improved performance in the Q-switched regime (10), but the size limitations to this technique pose a severe constraint.

We believe that in the past, epitaxial coatings have only been grown on crystalline samples. Both Textron and Northrop-Grumman Aerospace Systems are now using ceramic YAG slabs. Engineering of ceramics to include doped and undoped regions has been attempted, but is not widely used (11). It was unlikely that an epitaxial film could be grown on a ceramic YAG sample, but we thought it important to verify. Unfortunately, the first attempt failed, and no further attempts were made, there being no reasonable parameter to vary.

Hybrid Yb:YAG edge-pumped microchip lasers with a doped core and an undoped cladding have also been fabricated in the past. A 300 W continuous wave (cw) laser output has been obtained from a 5-mm diameter, 300- μm thick disk with a crystalline core and a ceramic

cladding (12). 414 W cw was later obtained from a 3.7-mm diameter, 200- μ m thick disk with a doped ceramic core and an undoped ceramic cladding (13).

2. Description

The power in the fundamental transverse electromagnetic mode (TEM_{00}) mode of a cavity is concentrated on axis, whereas the power in a WGM is highest at the periphery of the rod (figure 1). It is certain that an undoped cladding will suppress the WGM. It is not known how thick the cladding has to be or whether the interface quality will be sufficient to avoid loss for the pump beam. We planned to test an Er:YAG rod coated with undoped YAG to determine if the parasitic modes are suppressed, and compare the threshold and slope efficiency with an identical rod, without the cladding. Part of the cladding will then be ground away, the rod repolished, and the measurements repeated until the minimum thickness is determined.

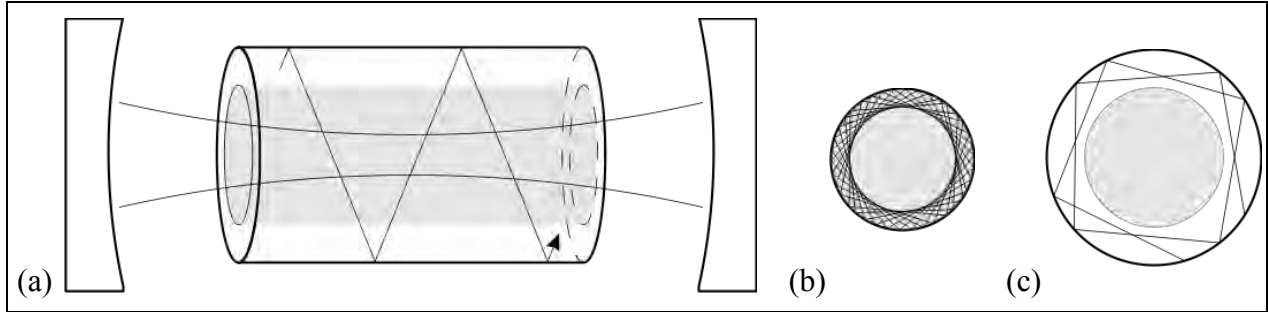


Figure 1. (a) An end-pumped clad rod in a laser cavity. The laser oscillation is a mode of the cavity, the pump beam is wave guided by TIR at the outer surfaces of the rod. (b) Rod cross section showing the whispering gallery modes that occupy $\sim 50\%$ of the volume for the case of an unclad YAG rod immersed in water. (c) In a rod clad with undoped material, the WGM will be suppressed because the gain is zero.

Liquid phase epitaxy (LPE) was successfully performed on a 3-mm diameter Er:YAG rod (figure 2) via flux growth over a period of seven days (14). The as-grown cladding is 1.5–2 mm thick. The interface between the “seed” rod and the cladding is practically invisible. A multi-faceted cross-section developed because of the anisotropic growth rates. The facets were of high quality, and we expected high efficiency wave-guiding of the pump beam without any further polishing. An anti-reflection coating was deposited on each end of the sample cut to a length of 26 mm. Lasing measurements were carried out on the sample at this stage, but were superseded by more accurate measurements made after the rod was ground and polished to a 6-mm diameter cylinder.

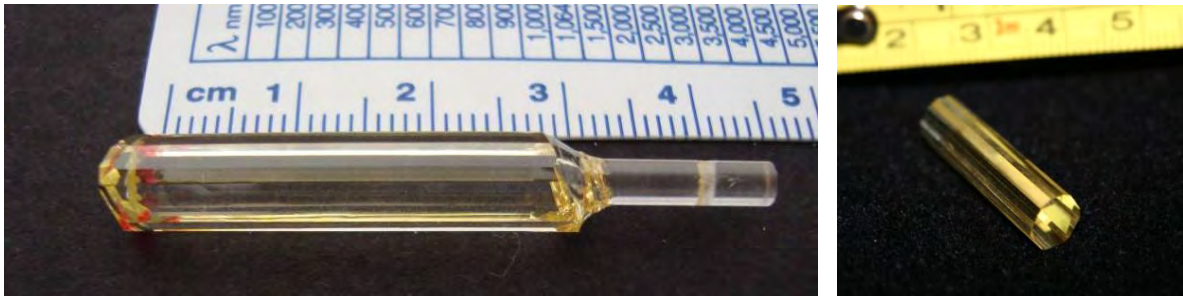


Figure 2. Er:YAG rod, 3 mm diameter, clad with ~2 mm of undoped YAG. (left) as-grown. (right) cut and polished.

3. Task 1–LPE on Single Crystal Er:YAG

The goals of this task were to:

- a. Image the whispering gallery modes that build up inside an unclad Er:YAG rod.
- b. Measure the transmission loss in a clad rod, due to scattering from the buried interface.
- c. Characterize the lasing threshold and slope efficiency of a clad rod, and compare with an unclad control rod of the same diameter for a series of different cladding thicknesses.

The first step was to design and fabricate two laser heads: one for the clad rod and one for the unclad rod. The outside diameter located the head inside a Thorlabs 30-mm cage in such a way that the heads could be easily interchanged. The cage also held the output coupler and sometimes the rear reflector. Several spacers, endcaps, and O-rings allowed the head to accommodate rods of different diameter (figure 3). During lasing experiments, the head was placed in a cavity formed by a high reflector and an output coupler (figure 4). The cavity was later extended to accommodate a diffuse reflector for measuring the transmitted pump power.

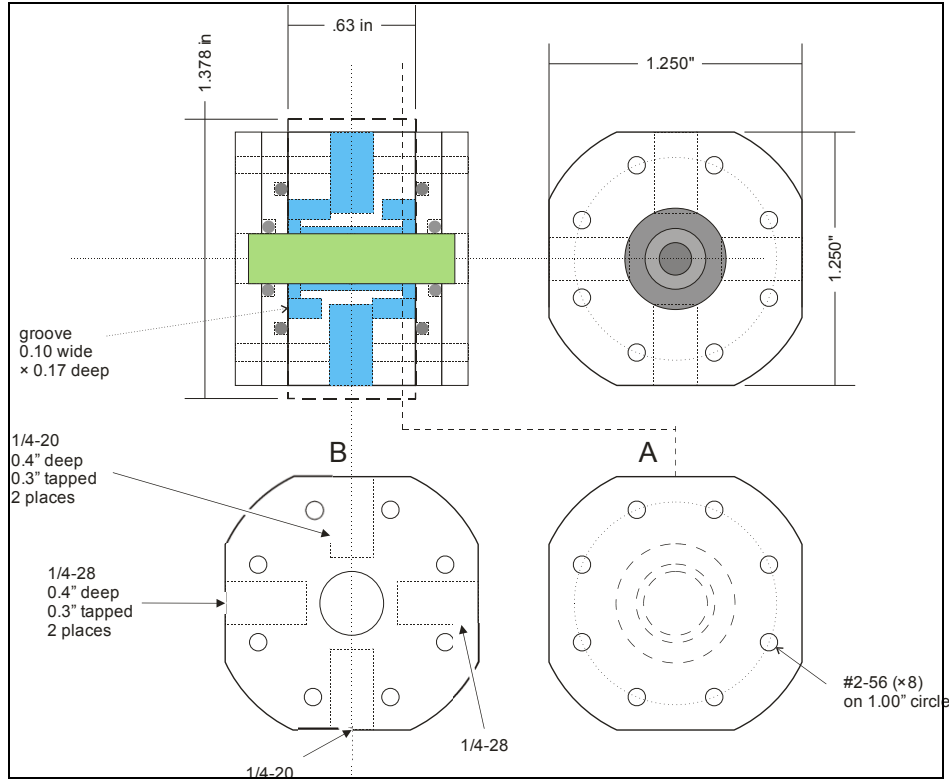


Figure 3. Drawing of laser head designed to accommodate rods of diameter 3–6 mm.

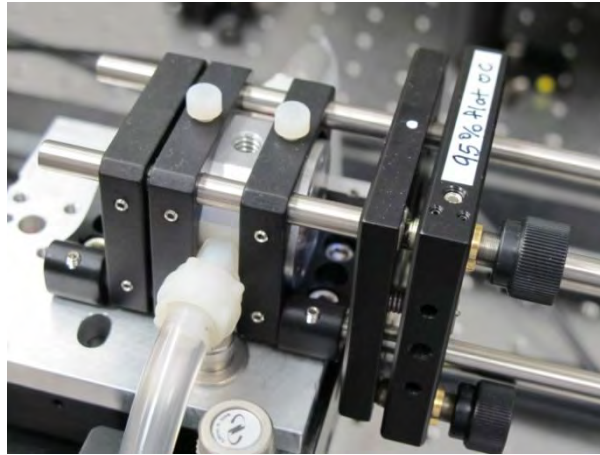


Figure 4. Laser cavity formed by high reflector, laser head, and output coupler.

Normally the WGM are confined to the rod by total internal reflection at the barrel surface. Some of the WGM light, however, will scatter from defects in the rod and exit, perhaps revealing the mode profile inside the rod. Following this idea, we pumped one end of the clad and unclad rods, without putting them in a cavity, and imaged the other end with a charge coupled device (CCD) camera sensitive at $1.6\ \mu$ (15). Long-wave-pass filters were used to block the 1532 nm

pump. Various patterns were observed, but they were qualitatively different from the WGMs we anticipated (figure 5).

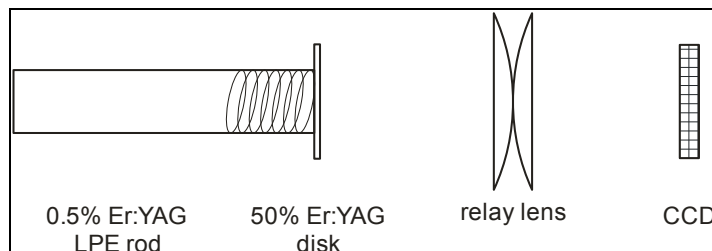


Figure 5. Side view of rod with WGM, upconversion disk, imaging optics, and digital camera.

At the end faces, the WGM typically undergo total internal reflection, unless the rod end is flared. Rods have also been tapered along their entire length to force the WGM to quickly exit the rod (5). We made several attempts to image the WGM by frustrating the total internal reflection (TIR) at the rod ends. Fifty percent-doped Er:YAG disks were placed against the exit face, with index oil in the gap, but nothing that evoked WGM was seen under pumping conditions (figure 6).

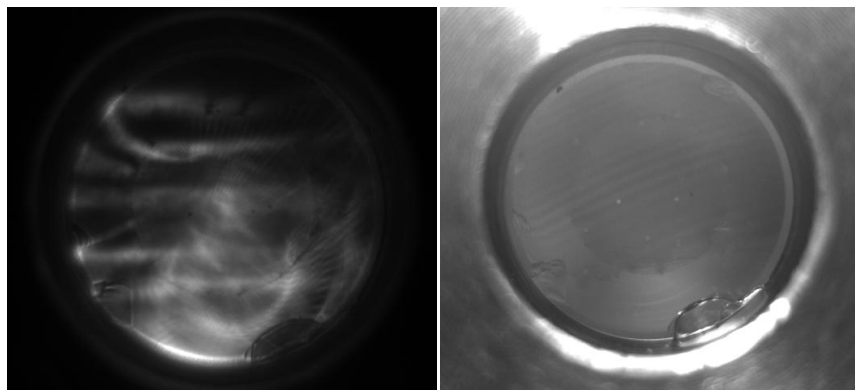


Figure 6. Images of the LPE rod face. (a) Fluorescence emitted from the rod when it is pumped at 1532 nm. The emission is transmitted through a long-wave pass filter. (b) Image taken with room light, showing the core (central darker region), cladding (with small chips), and laser head.

It was preferable to take data under conditions that approximate the steady-state in order to compare with theory at a later time. Rather than risk the damage that could occur when pumping cw with 300 W of average power, we used “quasi-cw” pumping with 10–50 ms pulses at a repetition rate low enough to keep the average power at ~30 W. To optimize the overlap of the 1532 nm pump (16) spectrum threshold and the Er absorption line, we used an external 1-mm-thick volume Bragg grating (VBG) (17) with a reflectivity of 20% to narrow the pump spectrum. To achieve steady-state conditions, it is necessary to avoid chirping of the pump diode during the 20–50 ms current pulse. This was accomplished by carefully adjusting the angle of the VBG while looking at a spectrum of the output, in order to optimize feedback into the laser. Under

these conditions, P_{out} rapidly reached a steady-state value, and we were able to acquire reliable P_{out} vs. P_{in} data. P_{in} was varied by rotating a $\lambda/2$ plate at a uniform rate with a computer-controlled stepper motor. The current pulses were maintained at 100 A so that the pump spectrum and spatial intensity distribution remained constant.

A meaningful comparison between the two rods has to be made on the basis of absorbed rather than incident pump power. The absorbed pump power was determined by measuring the incident and transmitted pump during lasing (figure 7), and taking the difference. Several different experimental configurations were tried. The best data was taken when the transmitted pump was measured by collecting some of the diffuse reflection from a 2-mm-thick sheet of sintered teflon (18) placed in the cavity, with a hole to pass the intracavity beam.

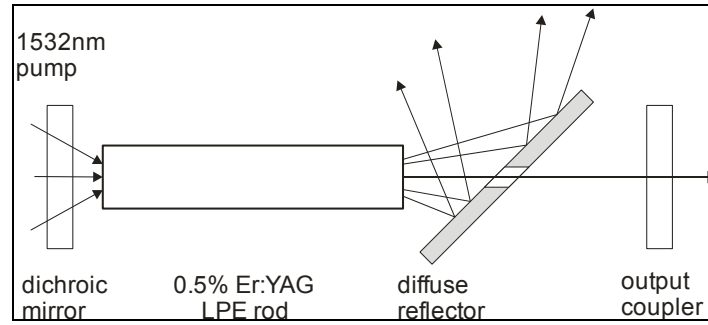


Figure 7. Geometry for measuring transmitted pump power during lasing.

A plot of P_{out} vs. P_{in} for an output coupler reflectivity of 0.98 shows that the unclad rod has both a lower threshold and a higher slope efficiency (figure 8), contrary to expectations. The same is true for all other output couplers, as well (figure 9). To check repeatability, the experiment was re-aligned from the beginning two days later, and the agreement was reasonable (figure 10).

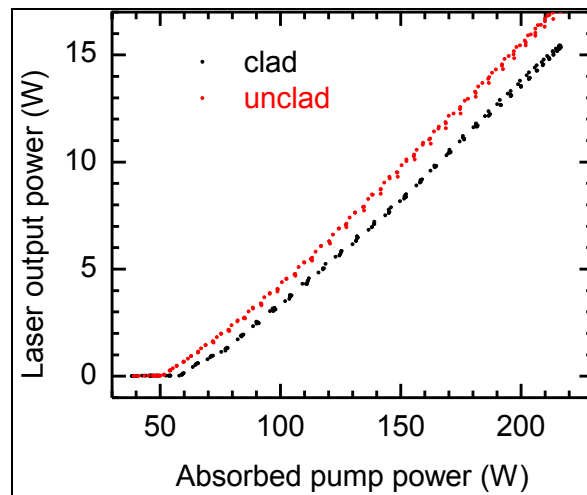


Figure 8. Laser output power vs absorbed pump power at $R=0.98$, for clad and unclad rods.

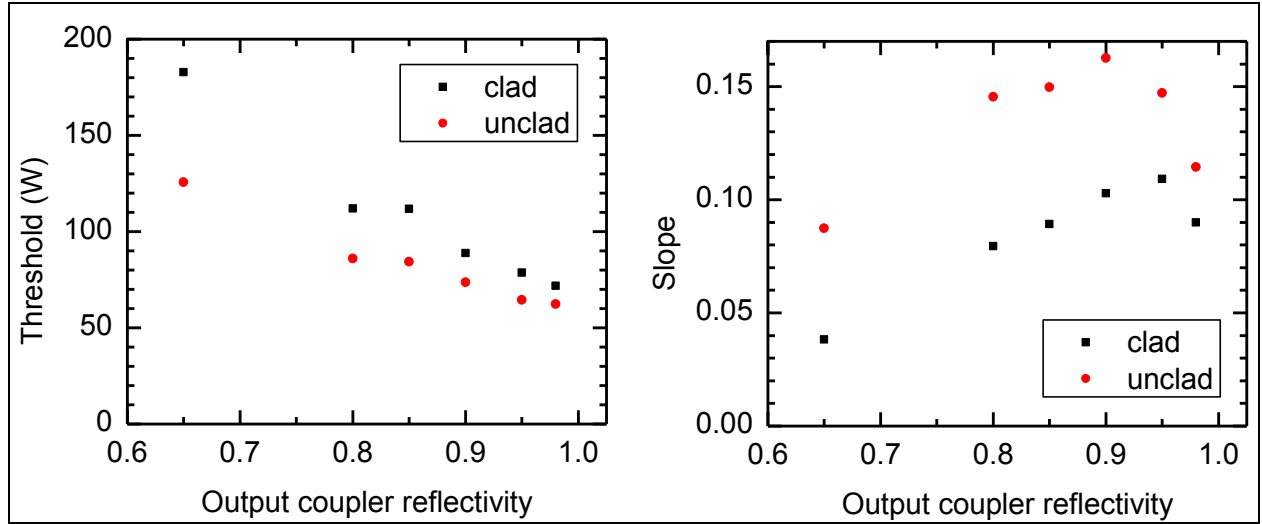


Figure 9. (left) Threshold absorbed pump power vs. output coupler reflectivity for clad and unclad rods. (right) Slope efficiency vs. output coupler reflectivity. Data recorded on 8 Feb.

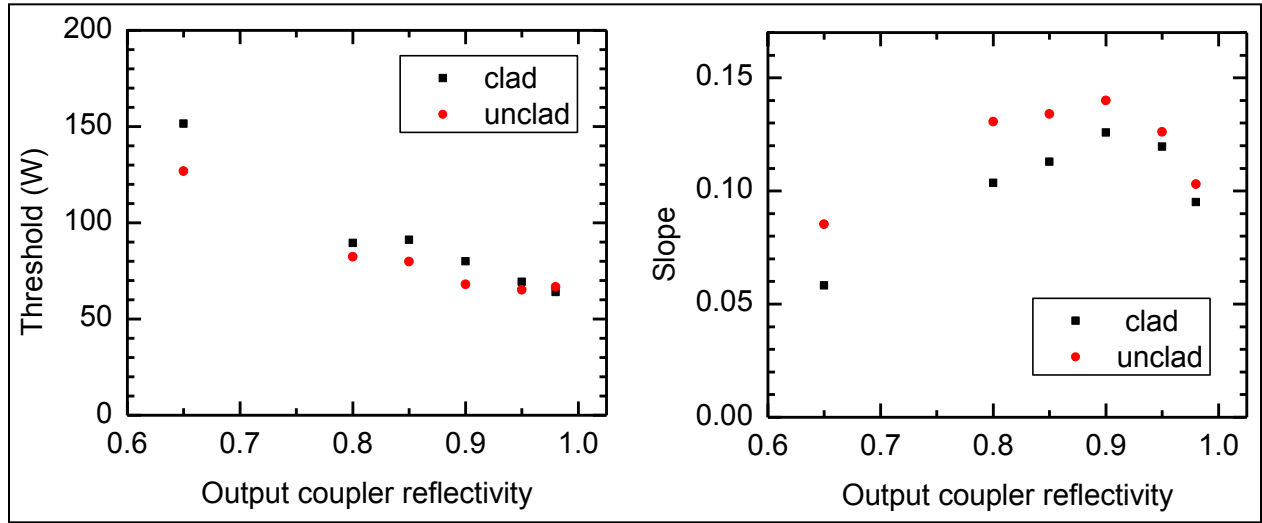


Figure 10. Same as figure 9, except experiment repeated on 10 Feb.

In the face of this negative result, we did not pursue the original plan of grinding the rod to explore thinner cladding layers. If the thickest cladding does not show any improvement over the unclad rod, there is no reason to believe that an intermediate thickness would.

Subsequent to the lasing experiments, to diagnose the problem, we imaged the rod cross-section in visible light using an electronic flash (figure 11). The images reveal an unexpected hexagonal pattern of yellow spokes emanating from the core, not readily visible to the naked eye, and probably due to the incorporation of lead oxide (PbO) flux during the epitaxy. We believe this explains the poor performance of the clad rod. A series of ~24 inclusions at the interface, running the length of the rod, which we had already observed by eye, also contribute to the poor performance.

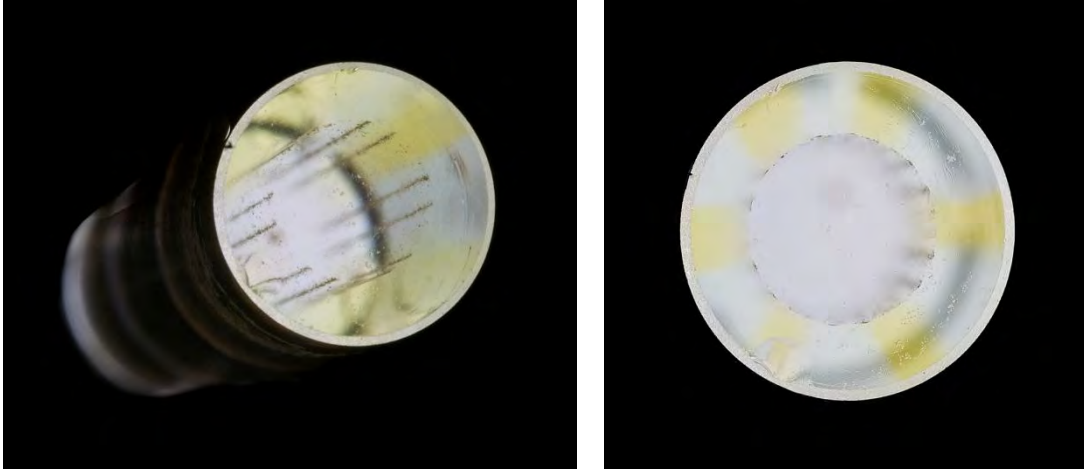


Figure 11. Images of the rod taken with a digital camera and electronic flash.

To determine if the yellow regions absorb pump light, photographs were taken using the collimated output of a 1532 nm laser diode, and the infrared (IR)-sensitive CCD. The images do not reveal the six-fold spoke structure (figure 12), so the reason for the poor performance is still unclear.

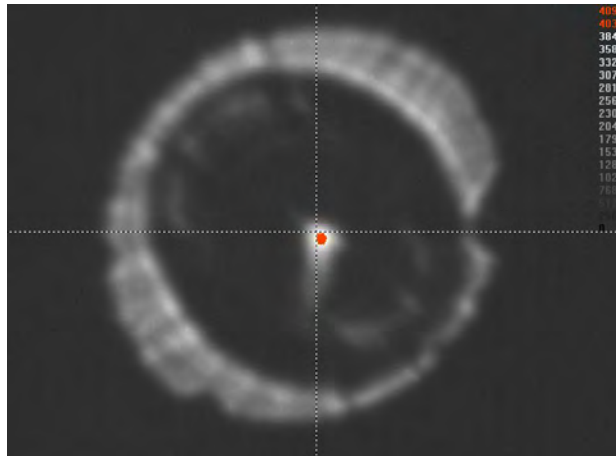


Figure 12. Projection image of the LPE rod taken with collimated 1532 nm light passing through the rod and then incident on the camera, with no focusing lens. The central hot spot is an interference effect.

4. Task 2—Simulation

The goal of this task was to model the propagation of light inside a multilayer rod, normal to the rod axis, to determine the minimum cladding thickness necessary to suppress the WGM.

Matlab software was written to determine how much the gain of the various transverse modes, including the WGM, would be affected by an undoped cladding on the outside of the gain region. First, the modes had to be calculated for a circular dielectric waveguide, e.g., an Er:YAG rod ($n_1 = 1.8$) in water ($n_2 = 1.33$). The numerical aperture (NA) is given by $NA^2 = n_2^2 - n_1^2$, and is equal to $NA = 1.21$. For a rod of even very modest radius $a = 0.2\text{mm}$, the normalized frequency of the highest confined given by $V = 2\pi a NA / \lambda \approx 470$. Thus, the number of confined modes is $V^2/2 = 2.2 \times 10^5$. A plot of V for each allowed HE_{lm} mode has the $HE_{1,1}$ mode at the vertex and the WGM running up the right hand side (figure 13). To illustrate the effect of a cladding on the gain, the following figures show the relevant fields for the fundamental mode ($EH_{1,1}$), the $HE_{1,1}$ mode, one mode along the left hand edge ($HE_{1,15}$), and several WGM along the right hand edge.

The four relevant field components for the $HE_{1,1}$ (fundamental) mode are shown in figure 14, as well as the z component of the Poynting vector. The overlap integral of the $HE_{1,1}$ mode with gain regions of different diameters can be ready by eye from a graph of the spatial integral of the z component of the Poynting vector. One can see that to halve the gain of the $HE_{1,1}$ mode, the outer 58% of the rod has to be undoped (figure 14). To halve the gain of the $EH_{1,1}$ mode, the outer 37% has to be undoped (figure 15). To halve the gain of the $HE_{1,15}$ mode, the outer 50% has to be undoped (figure 16). To halve the gain of the $HE_{10,1}$ mode, the outer 30% has to be undoped (figure 17). To halve the gain of the $EH_{20,1}$ mode, the outer 30% has to be undoped (figure 18). To halve the gain of the $HE_{30,1}$ mode by half, only the outer 4.6% has to be undoped (figure 19). This is the basis for believing that a *thin* undoped cladding would be sufficient to suppress the WGM.

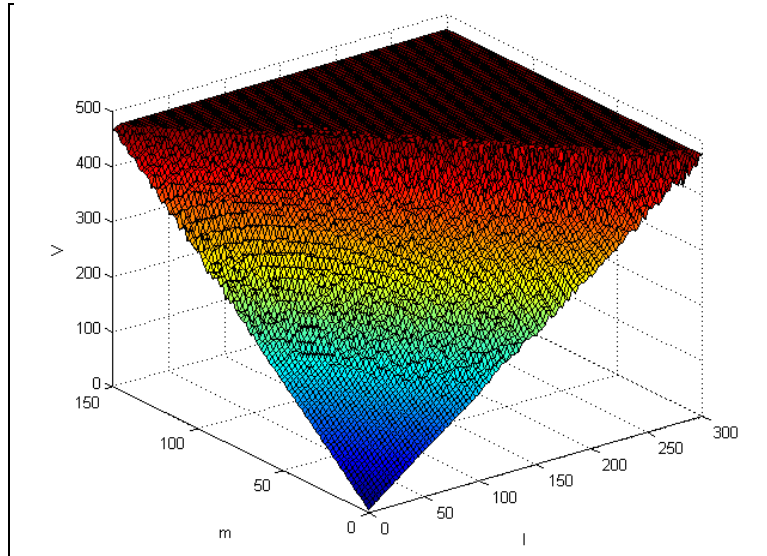


Figure 13. Graph showing which EH_{lm} modes are supported by an 0.2 mm diameter YAG rod in H_2O ($V = 471$).

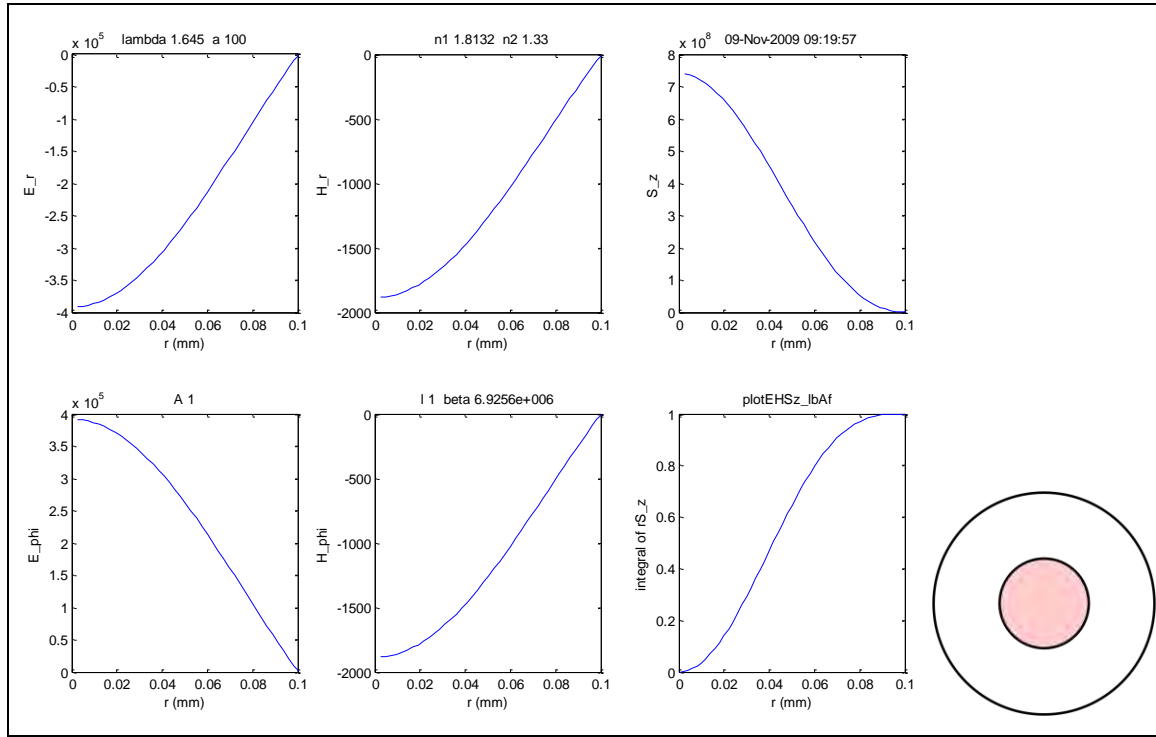


Figure 14. Fields E_r , E_{ϕ} , H_r , H_{ϕ} , and S_z associated with the $HE_{1,1}$ (fundamental) mode of a 200μm diameter YAG rod in water. The 2D integral of the Poynting vector is shown in the lower right hand graph. The diagram shows the 58% cladding thickness required to halve the gain.

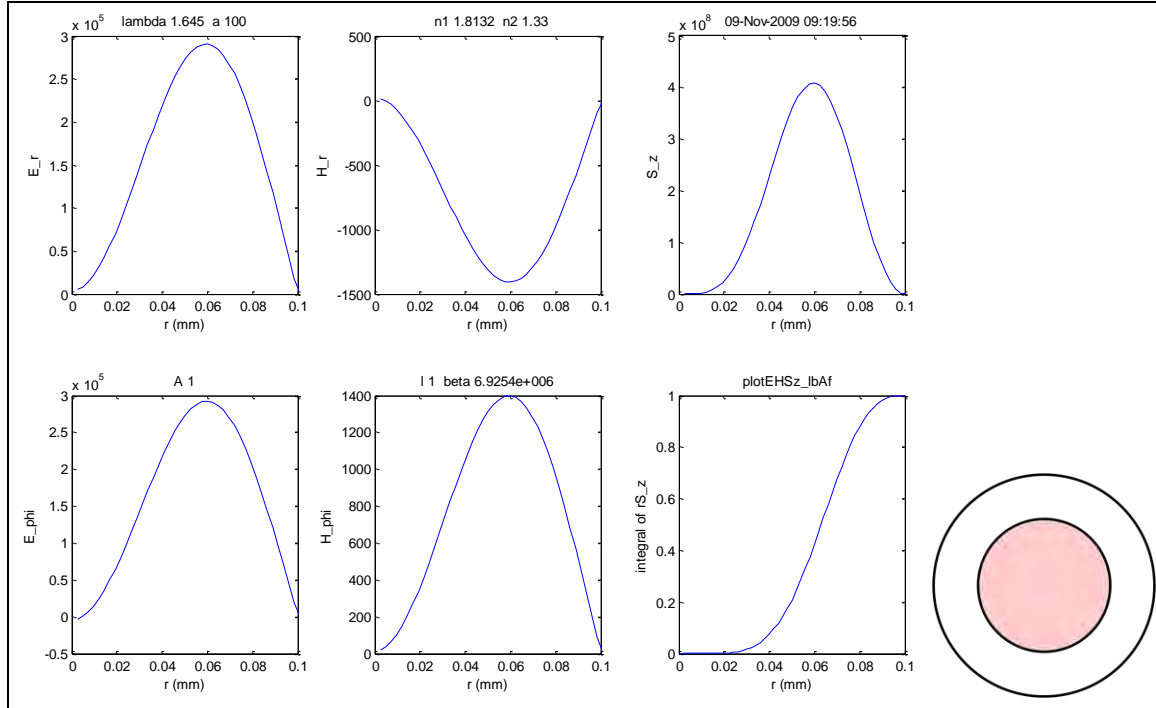


Figure 15. Fields associated with the $EH_{1,1}$ mode of the same rod, the 2D integral of the Poynting vector, and the 37% cladding thickness required to halve the gain.

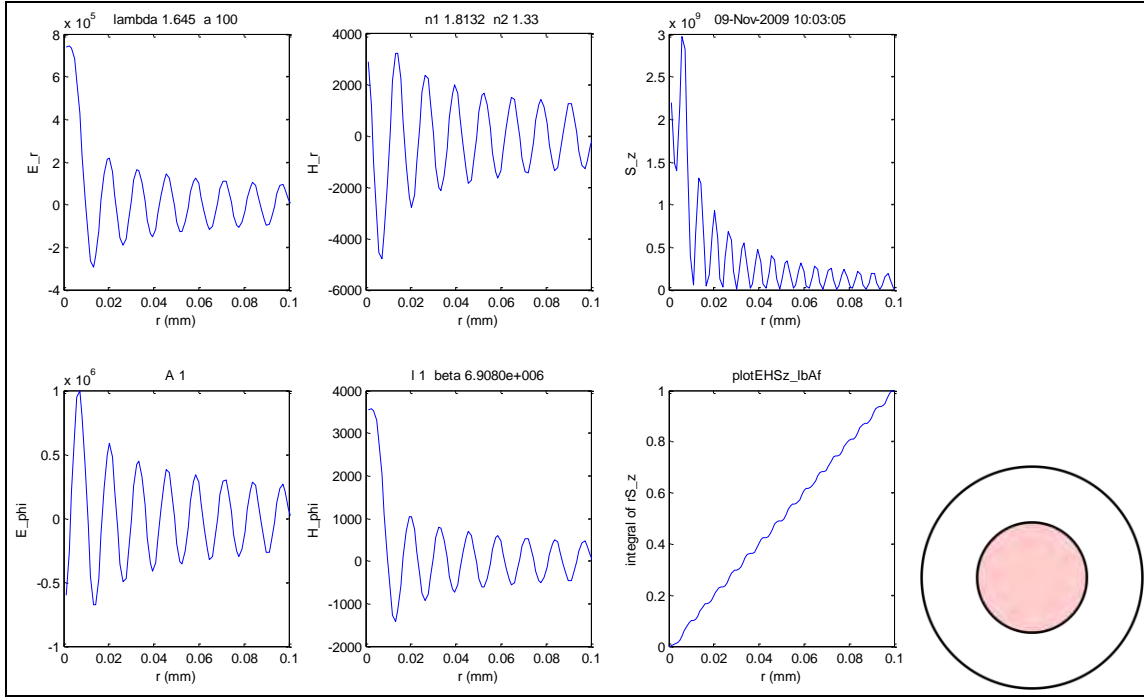


Figure 16. Fields associated with the $HE_{1,15}$ mode, the 2D integral of the Poynting vector, and the 50% cladding thickness required to halve the gain.

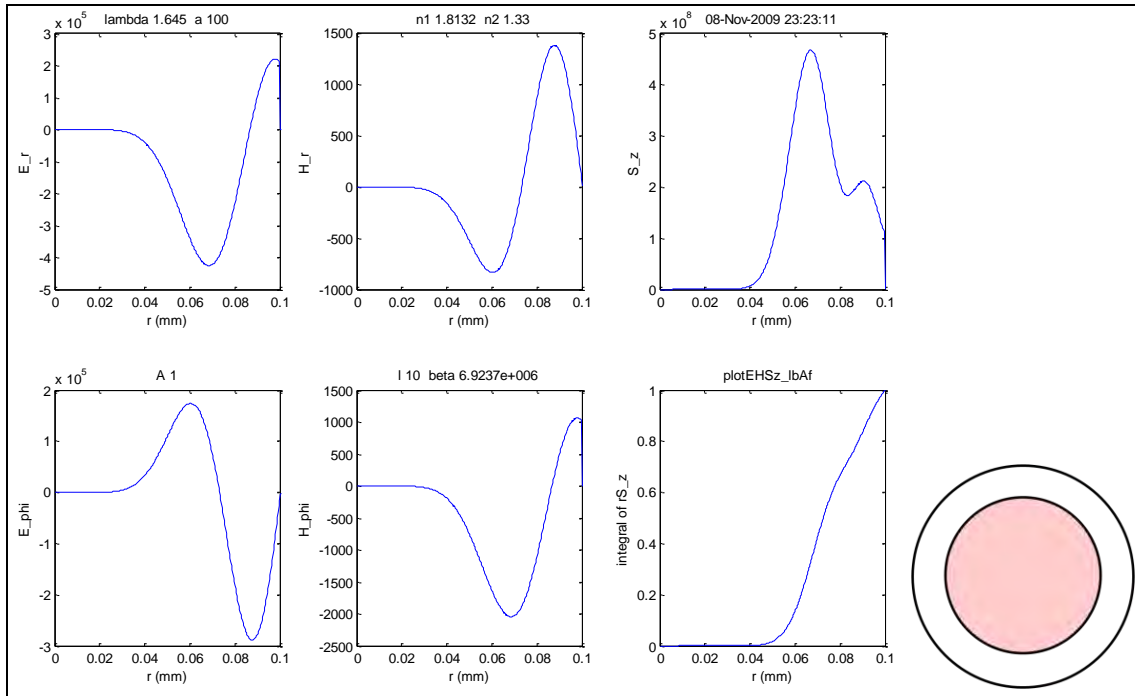


Figure 17. Fields associated with the $HE_{10,1}$ mode, the 2D integral of the Poynting vector, and the 28% cladding thickness required to halve the gain.

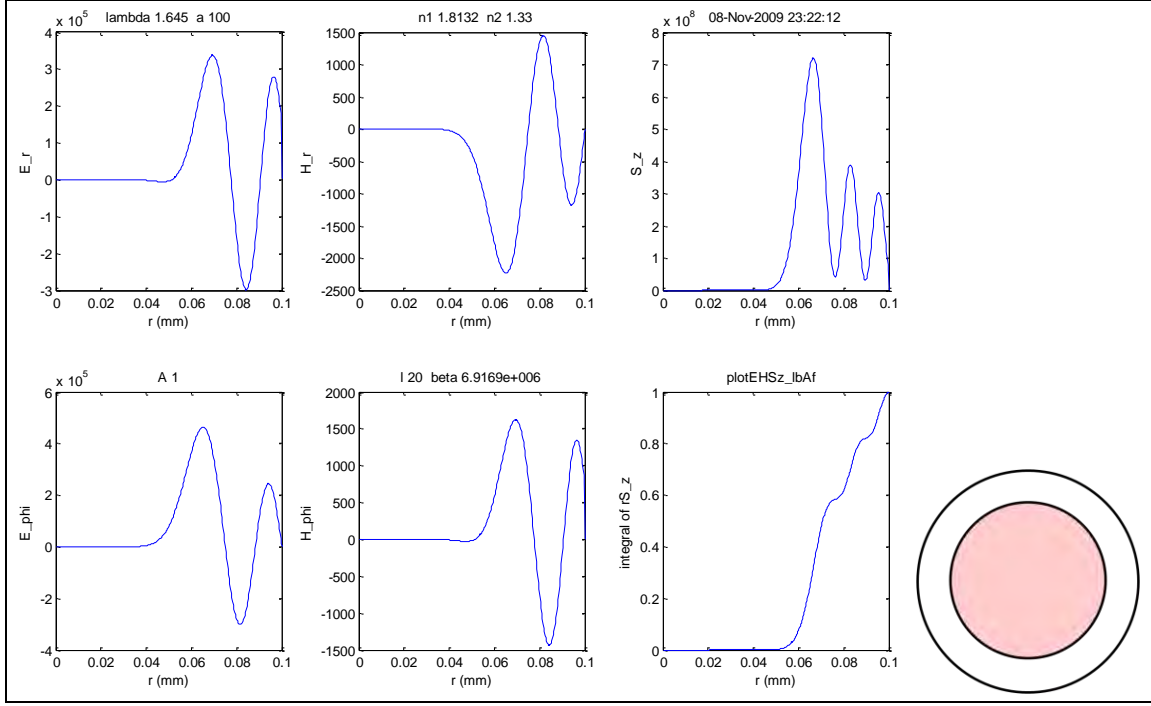


Figure 18. Fields associated with the $EH_{20,1}$ mode, the 2D integral of the Poynting vector, and the 29% cladding thickness required to halve the gain.

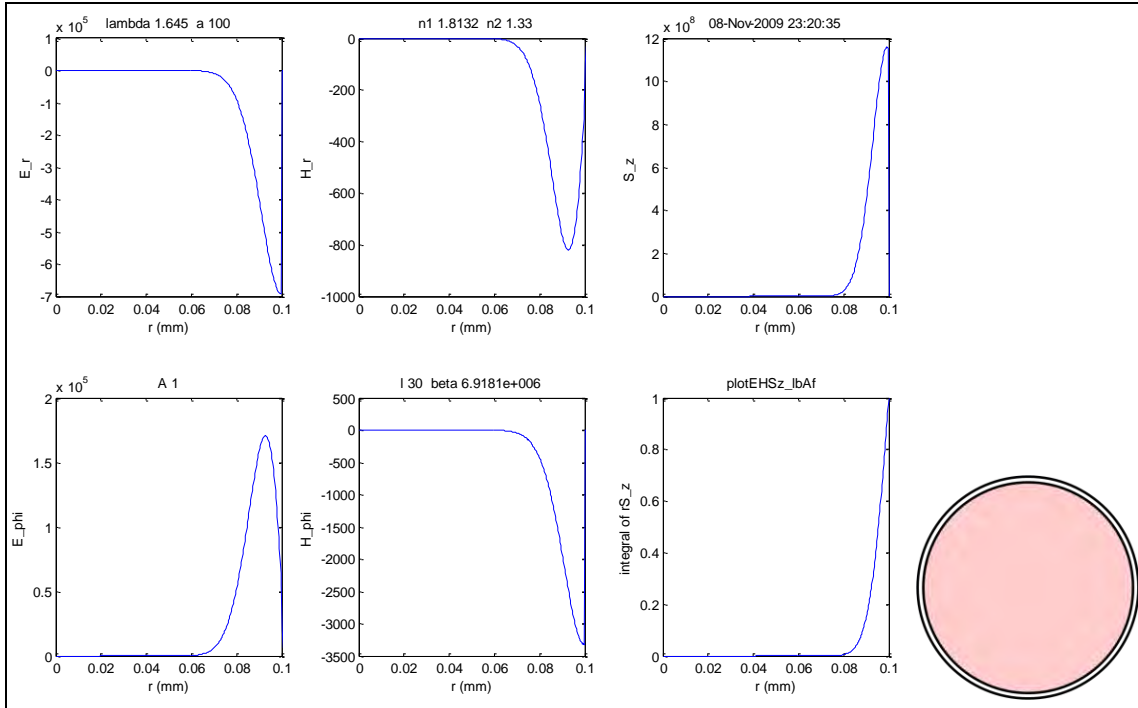


Figure 19. Fields associated with the $HE_{30,1}$ mode, the 2D integral of the Poynting vector, and the 4.6% cladding thickness required to halve the gain.

The High Energy Laser Joint Technology Office (HEL-JTO) committee asked that we look into the possibility of using LPE to grow doped YAG single crystal slabs of the size used in the JHPSSL program. The following is a summary of what Mark Randles at Northrup-Grumman Synoptics said.

The current setup at Synoptics—i.e. a 5-in. diameter crucible, 60–70 mm deep—is not adequate for growing volumes of more than 0.5–1.0 cm³, e.g. a 1 mm thickness on a 1-in. diameter substrate. The volume is limited because the melt is 90% PbO, and the YAG simply runs out. One could start with a higher concentration of YAG, but then the melting point would be higher, and the vapor pressure of Pb would become too high. The growth starts from a supersaturated solution of PbO and YAG. The addition of boron oxide stabilizes the melt against crystallization, by making it more viscous, until it comes in contact with a seed. As the YAG is depleted during growth, the melt temperature is lowered to remain supersaturated. The growth rate slows as the YAG is depleted. If the sample were to be removed and the melt replenished, the sudden change in growth rate when the sample is re-immersed would create a visible interface.

The upshot is that growth of single-crystal slabs of the size used in the JHPSSL program is not feasible with crucibles of the present size. Even growing a cladding layer on a full-sized slab would require a larger crucible. No *fundamental* obstacles are foreseen, however.

Concerning the loss measurements that Synoptics may have made on their epitaxial material, they have not made any. The microchip lasers made by Leica and Concepts Research are only about 1 mm thick, so current levels of loss are not a factor. Synoptics is mainly concerned with using the height of the Nd and Cr absorption peaks to control the level of doping. They obviously try to avoid inclusions of flux, and have not done any spectroscopy of them.

One advantage of LPE vs. Czochralski is the higher doping—2.5–3.0% vs. 1.1–1.2%. The thin disk laser manufacturers do not use LPE-grown material, although it might seem like a reasonable thing to do. Arguing against epitaxy is the need to evaporate a multi-layer reflective coating onto the back side of the thin disk, which would interrupt the epitaxy. Another reason not to use epitaxy is that they prefer to bond (or glue) the YAG to a more thermally conductive material, e.g. sapphire, for heat removal.

5. Task 3—LPE on Ceramic

The goals of this task were to:

- a. Obtain test samples of ceramic YAG, and coat one face of each via LPE.
- b. Measure the scattering loss at the buried interface.

In the past, epitaxial coatings have generally been grown on crystalline samples. We also investigated LPE growth on a ceramic sample, because high power slab lasers are now typically ceramic. Engineering of ceramics to include doped and undoped regions has been attempted, but is not widely used (19). It was unlikely that an epitaxial film could be grown on a ceramic YAG sample, but we thought it important to verify. Unfortunately, the first attempt failed (figure 20), and no further attempts were made, there being no reasonable parameter to vary. The optical quality was so poor that no lasing or even transmission measurements were attempted.



Figure 20. Photo of a ceramic rod from Konoshima after an attempt at liquid phase epitaxy.

6. Conclusion

The concept of growing an undoped epitaxial layer onto the outside of a *single-crystal* YAG rod was a reasonable approach to suppressing the parasitic WGM that can occupy 50% of the volume of the rod. Liquid phase epitaxy was used to grow a ~2-mm-thick undoped layer on a 3-mm Er-doped rod. The clad rod failed to show improved performance compared to an unclad rod. Photographic evidence leads us to believe that the failure was due to the incorporation of PbO flux into the epitaxial layer, which then absorbed pump light. The concept of growing an epitaxial layer onto a *ceramic* substrate had less chance of success, but was considered prudent to try, given the importance of ceramic slabs to 100 kW class solid-state lasers. A single attempt was made; it failed.

7. References

1. Linn, J.; Free, J. Effect of Trapped Light on the Output of a Ruby Laser. *Appl. Opt.* **1965**, *4*, 1099–1101.
2. Galoyan, K. V.; Kahchatryan, K. U. *Sov. J. Quantum Electron.* **1974**, *4*, 260.
3. Bibeau, C., et al. High-average-power 1- μm Performance and Frequency Conversion of a Diode-end-pumped Yb:YAG Laser. *IEEE J. Quantum Electronics* **1998**, *34*, 2010.
4. Honea, E. C., et al. High-power Dual-rod Yb:YAG Laser. *Optics Lett.* **2000**, *25*, 805.
5. Beach, R. J., et al. High-average-power Diode-pumped Yb:YAG Lasers. LLNL preprint UCRL-JC-133848, submitted to the Int'l Forum on Advanced High-Power Lasers and Applications, Suita, Japan, Nov. 1-5, 1999.
6. Glaze, J. A.; Guch, S.; Trenholme, J. B. Parasitic Suppression in Large Area Nd:glass Disk Laser Amplifiers. *Appl. Opt.* **1974**, *13*, 2808–2811.
7. Injeyan, H. Northrop Grumman Space Technologies, private communication.
8. Trainor, D. Textron, private communication.
9. Adhesive Free Bonding®, Onyx Optics, 6545 Sierra Lane, Dublin, Calif. 94568.
10. Lucianetti, A., et al. Beam-quality Improvement of a Passively Q-switched Nd:YAG Laser with a Core-doped Rod. *Appl. Opt.* **1999**, *38*, 1777–1783.
11. Kracht, D.; Freiburg, D.; Wilhelm, R.; Frede, M.; Fallnich, C. Core-doped Ceramic Nd:YAG Laser. *Optics Express* **2006**, *14*, 2690.
12. Tsunekane, M.; Taira, T. 300 W Continuous-wave Operation of a Diode Edge-pumped, Hybrid Composite Yb:YAG Microchip Laser. *Opt. Lett.* **2006**, *31*, 2003–2005.
13. Tsunekane, M.; Taira, T. High-power Operation of Diode Edge-pumped, Composite All-ceramic Yb:YAG Microchip Laser. *Appl. Phys. Lett.* **2007**, *90*, 121101.
14. Randles, Mark. Northrop-Grumman Synoptics, 1201 Continental Blvd., Charlotte, NC 28273.
15. Spiricon model SCOR-1550.
16. Stack of ten InGaAs diode bars from Princeton Lightwave, Inc., 2555 Route 130 South, Cranbury, NJ 08512.
17. PD-LD, 30-B Pennington-Hopewell Rd., Pennington, NJ 08534.
18. Spheroptics, now Labsphere, 231 Shaker Street, North Sutton, NH 03260.
19. Kracht, D.; Freiburg, D.; Wilhelm, R.; Frede, M.; Fallnich, C. Core-doped Ceramic Nd:YAG Laser. *Optics Express* **2006**, *14*, 2690.

NO. OF COPIES	ORGANIZATION
1 ELEC	ADMNSTR DEFNS TECHL INFO CTR ATTN DTIC OCP 8725 JOHN J KINGMAN RD STE 0944 FT BELVOIR VA 22060-6218
1 CD	OFC OF THE SECY OF DEFNS ATTN ODDRE (R&AT) THE PENTAGON WASHINGTON DC 20301-3080
1	US ARMY RSRCH DEV AND ENGRG CMND ARMAMENT RSRCH DEV & ENGRG CTR ARMAMENT ENGRG & TECHN LGY CTR ATTN AMSRD AAR AEF T J MATTS BLDG 305 ABERDEEN PROVING GROUND MD 21005-5001
1	US ARMY INFO SYS ENGRG CMND ATTN AMSEL IE TD A RIVERA FT HUACHUCA AZ 85613-5300
1	COMMANDER US ARMY RDECOM ATTN AMSRD AMR W C MCCORKLE 5400 FOWLER RD REDSTONE ARSENAL AL 35898-5000
1	US GOVERNMENT PRINT OFF DEPOSITORY RECEIVING SECTION ATTN MAIL STOP IDAD J TATE 732 NORTH CAPITOL ST NW WASHINGTON DC 20402
1	U.S. NAVAL ACADEMY PHYSICS DEPARTMENT ATTN CARL E. MUNGAN ANNAPOLIS, MARYLAND 21402-1363
16	US ARMY RSRCH LAB ATTN IMNE ALC HRR MAIL & RECORDS MGMT ATTN RDRL CIO LL TECHL LIB ATTN RDRL CIO MT TECHL PUB ATTN RDRL SEE O J WHITE (10 HCS) ATTN RDRL SEE O N FELL ATTN RDRL SEE O D SMITH ATTN RDRL SEE G WOOD ADELPHI MD 20783-1197